Thermochimica Acta, 198 (1992) 313–328
Elsevier Science Publishers B.V., Amsterdam

The structure and influence of ferric oxide on the properties of $3CaO \cdot 3Al_2O_3 \cdot BaSO_4$

Dun Chen [a], Xiuji Feng [b] and Shizhong Long [b]

[a] *Department of Chemistry, The University of Toledo, OH 43606 (USA)*
[b] *Department of Materials Sciences, The Wuhan University of Technology, Hubei, 430070 (People's Republic of China)*

(Received 12 August 1991)

Abstract

The structure of $3CaO \cdot 3Al_2O_3 \cdot BaSO_4$ was determined by computer programs which are based on the single-crystal structure of $3CaO \cdot 3Al_2O_3 \cdot CaSO_4$ as T^5-I23; $a = b = c = 9.303 \pm 0.002$ Å, $\alpha = \beta = \gamma = 90°$, density 3.01 g cm^{-3}. The maximum amount of ferric oxide in $3CaO \cdot 3Al_2O_3 \cdot BaSO_4$ by replacement of Al_2O_3 was determined by electron microprobe analysis which led to the proposed formula, $3CaO \cdot 2.71Al_2O_3 \cdot 0.29Fe_2O_3 \cdot BaSO_4$.

The physical properties of the compound with and without ferric oxide were measured together with the analysis of the hydration process and products using XRD, DTA and equipment to determine the heat of hydration, etc. The results show that the presence of barium sulfate has the ability to prevent the transformation of calcium aluminate decahydrate ($CaO \cdot Al_2O_3 \cdot 10H_2O$) to tricalcium aluminate hexahydrate ($3CaO \cdot Al_2O_3 \cdot 6H_2O$). Also there is a new phase present in the hydration products which has a DTA peak similar to that of the calcium monosulfoaluminate hydrate ($3CaO \cdot Al_2O_3 \cdot CaSO_4 \cdot 12H_2O$).

INTRODUCTION

In reports published on the $CaO–Al_2O_3–CaSO_4$ system during the 1960s, the compound $3CaO \cdot 3Al_2O_3 \cdot CaSO_4$ was found and identified. Because this compound has the property of expansion after it hydrates, it became very important in the cement industry: it offered the possibility of compensating for a disadvantage of cements, namely that shrinkage after hardening occurs which can cause fracture of fabricated components. It thus became the main component of expansive cements.

According to the research reported by Teoreanu et al. [1], there should be other derivatives of $3CaO \cdot 3Al_2O_3 \cdot CaSO_4$. They claim to have found some compounds of formulae $3CaO \cdot Al_2O_3 \cdot M_x(SO_4)_y$ ($M = Mg^{2+}$, Sr^{2+}, Ba^{2+}, Fe^{3+}, Al^{3+}) by heating mixtures of $M_x(SO_4)_y$ with $CaCO_3$ and Al_2O_3

Correspondence to: Dun Chen, Department of Chemistry, University of Toledo, OH 43606, USA.

at 1400°C for 4 h. From the most recent research [2] on the derivatives of $3CaO \cdot 3Al_2O_3 \cdot CaSO_4$ formed by substituting calcium sulfate with strontium sulfate or barium sulfate, it has been shown that Teoreanu et al. did not produce these compounds. These compounds can only be prepared at appropriate heating temperatures.

Using computer programs, the structure of $3CaO \cdot 3Al_2O_3 \cdot BaSO_4$ was determined from powder XRD: a very similar structure to that of $3CaO \cdot 3Al_2O_4 \cdot CaSO_4$ [2] was found. To further the investigations and to make it possible to produce a new kind of cement, Fe_2O_3 was introduced into $3CaO \cdot 3Al_2O_3 \cdot BaSO_4$. The properties of this series of compounds, which is called the BF system [a], are reported in this study. Also, by following the process of hydration more information is obtained and this helps to explain the properties of this series of compounds.

EXPERIMENTAL

Materials

Different ratios of the analytically pure chemicals calcium carbonate, aluminum oxide, barium sulfate and ferric oxide were used to obtain the appropriate mixtures calculated from the formula $3CaCO_3 \cdot (3-x)Al_2O_3 \cdot xFe_2O_3 \cdot BaSO_4$ where $x = 0$, 0.2, 0.4, 0.6, 0.8, 1.0. The symbols and compositions of the samples are shown in Table 1. The samples were ground and mixed thoroughly and the appropriate amount of water was added to form a compact about 10 mm thick and 20 mm in diameter under pressure. After sintering the samples in the form of wet compacts at appropriate temperatures for 4 h, they were cooled in air and ground again to obtain the final products which were stored in a desiccator.

The density of $3CaO \cdot 3Al_2O_3 \cdot BaSO_4$ was measured using an oil displacement method. The compressive strength of the samples was measured using neat paste in a small mould ($2 \times 2 \times 2$ cm^3) and a water to solid ratio (w/c) of 0.29. In order to investigate the possibility of producing a new kind of cement, calcium aluminate ($CaO \cdot Al_2O_3$) and calcium dialuminate ($CaO \cdot 2Al_2O_3$) were prepared by thoroughly mixing ground $CaCO_3$ and Al_2O_3, moulded to form wet compacts which were sintered at 1400°C for 4 h, cooled in air and finally ground to obtain the products. They were added to the $3CaO \cdot 3Al_2O_3 \cdot BaSO_4$. The two materials were mixed in a wt.% ratio of 50%. After curing for one day in a humidity chamber, the compacts were then cured in water at 25°C. The compressive strength was measured at 3, 7 and 28 days.

[a] In cement chemists' notation C = CaO, A = Al_2O_3, F = Fe_2O_3, H = H_2O.

TABLE 1

The compositions of the samples (wt.%)

Samples	$CaCO_3$	Al_2O_3	$BaSO_4$	Fe_2O_3
BF00	35.77	36.43	27.80	
BF02	35.28	33.54	27.43	3.75
BF04	34.81	30.73	27.05	7.41
BF06	34.35	27.99	26.70	10.96
BF08	33.90	25.32	26.35	14.42
BF10	33.46	22.73	26.01	17.80

The sample residues were immediately immersed in analytical grade ethanol to obtain the SEM pictures. To get more information on the hydration products, the residue was ground with analytical grade ethanol to pass a 180-mesh sieve, washed twice with analytical grade ethanol and acetone, heated under vacuum at 50–60°C for 2–3 h, and then heated at 60°C for 3 h. The products were stored in a desiccator.

All the surface area measurements were made using the Blain permeability apparatus.

Apparatus

From the powder XRD results, the structure of $3CaO \cdot 3Al_2O_3 \cdot BaSO_4$ was determined using computer programs. After collecting the diffraction data, the TREOR program was used to obtain the indices of each peak, the 9214 non-linear least-squares program was then run to modify them and, finally, the simulated structure of $3CaO \cdot 3Al_2O_3 \cdot BaSO_4$ was obtained by running the POWD12 program. The data collection took place at an acceleration voltage of 20 kV and a current of 100 mA with step scanning. All the data collection and calculation were done on the D/MAX-$\gamma\beta$ system.

After mixing the sample with appropriate amounts of α-Al_2O_3 powder, a thin layer was exposed using the HZG4-PC X-ray diffractometer to obtain the exact positions of peaks and then the Bragg equation was used to calculate the lattice constants. The parameters of the X-ray diffractometer were $2\theta = 1/100$ and the data collection interval was 2 s.

The determination of the maximum amount of solid solution was achieved using a JEOL electron microprobe analysis equipment, JXCA-733. The acceleration voltage was 200 kV and the diameter of the electron probe was about 5 μm.

The liberated heat of hydration at 30°C was measured using the Seteram microcalorimeter HT-1500 on a sample with $w/c = 10$.

DTA patterns were measured on Shanghai DTA equipment with the following parameters: sensitivity, 10 mV; heating rate, 10°C min^{-}. The temperature range was from room temperature to 600°C.

The SEM pictures were obtained using a JEOL ISI-SX-40 electron microscope. The acceleration voltage was 20 kV.

RESULTS AND DISCUSSION

Structure and the maximum solid solution

The X-ray powder diffraction results for $3CaO \cdot 3Al_2O_3 \cdot BaSO_4$ and $3CaO \cdot 3Al_2O_3 \cdot CaSO_4$ are shown in Tables 2a and 2b and the structure of $3CaO \cdot 3Al_2O_3 \cdot BaSO_4$ as calculated from the computer programs was T^5-I23, $a = b = c = 9.303 \pm 0.002$ Å, $\alpha = \beta = \gamma = 90°$. In addition, the coordinators of $3CaO \cdot 3Al_2O_3 \cdot BaSO_4$ are compared with those of $3CaO \cdot 3Al_2O_3 \cdot CaSO_4$ in Table 3.

From Table 3, it can be seen that there is a very small difference between the coordinators of these two compounds. Also by comparing the peaks of $3CaO \cdot 3Al_2O_3 \cdot BaSO_4$ with those of $3CaO \cdot 3Al_2O_3 \cdot CaSO_4$, there are fewer peaks in $3CaO \cdot 3Al_2O_3 \cdot BaSO_4$ which means that it has a lower symmetry. The reason for this is that the radius of barium is much larger than that of calcium; after barium atoms replace calcium atoms in $3CaO \cdot 3Al_2O_3 \cdot CaSO_4$, it alters the order of $3CaO \cdot 3Al_2O_3 \cdot CaSO_4$, making the structure is much more disordered.

The results of these experiments indicate that as the amount of ferric oxide in the BF system compounds (see Table 1) rises, the XRD peaks move to a lower angle which means that the lattice constant rises. When the amount of iron atoms in $3CaO \cdot 3Al_2O_3 \cdot BaSO_4$ reaches a maximum, the lattice constant of $3CaO \cdot 3Al_2O_3 \cdot BaSO_4$ with iron atoms will also reach a constant value which remains unchanged even with larger amounts

TABLE 2a

X-ray powder diffraction data of $3CaO \cdot 3Al_2O_3 \cdot BaSO_4$

No	Index	d (Å)	I/I_0	No	Index	d (Å)	I/I_0
1	200	4.659	10	9	420	2.079	2
2	211	3.801	100	10	332	1.983	3
3	220	3.290	15	11	422	1.899	4
4	310	2.943	15	12	510	1.825	7
5	222	2.658	25	13	440	1.645	6
6	321	2.485	11	14	530	1.595	8
7	400	2.326	6	15	600	1.550	10
8	411	2.192	50				

TABLE 2b

X-ray powder diffraction data of $3CaO \cdot 3Al_2O_3 \cdot CaSO_4$

No	Index	d (Å)	I/I_0	No	Index	d (Å)	I/I_0
1	321	4.915	8	15	732/651	2.335	1
2	400	4.613	2	16	800	2.302	4
3	411	4.321	4	17	811/741	2.261	3
4	422	3.752	100	18	554/653	2.194	2
5	440	3.249	9	19	822/660	2.168	20
6	530/433	3.152	3	20	831/750	2.130	3
7	532/611	2.987	3	21	840/743	2.034	3
8	620	2.911	7	22	910/833	2.032	3
9	541	2.837	2	23	921/761	1.984	2
10	444	2.653	30	24	664	1.960	2
11	710/550	2.603	2	25	884	1.877	3
12	721/633	2.505	3	26	941/853	1.856	2
13	642	2.455	7	27	862/1020	1.804	4
14	730	2.416	2	28	950/943	1.788	2

of iron atoms in the mixture. The results of the lattice constant determinations, which are shown in Table 4 and Fig. 1, indicate that in sample BF06, the iron atoms in the compound have reached the maximum amount, i.e. it is saturated with respect to iron. But from the XRD results on all BF system compounds, which are shown in Table 5, it can be seen that not all of the added ferric oxide stayed in the lattice of the compound, instead it always formed C_xAF_{1-x} (mainly in the C_2F form). To obtain the actual value of the amount of ferric oxide in $3CaO \cdot 3Al_2O_3 \cdot BaSO_4$, electron microprobe analysis was carried out on the BF06 and BF08 samples. The results are shown in Table 6. From this data and by calculation, the proposed formula of the maximum solid solution of Fe_2O_3 in $3CaO \cdot 3Al_2O_3 \cdot BaSO_4$ is $3CaO \cdot 2.71Al_2O_3 \cdot 0.29Fe_2O_3 \cdot BaSO_4$.

TABLE 3

Coordinators of $3CaO \cdot 3Al_2O_3 \cdot BaSO_4$ and $3CaO \cdot 3Al_2O_3 \cdot CaSO_4$

Elements [a]	No	x/a	y/b	z/c	No	x/a	y/b	z/c
Ca^1	6	0.1904	0.1904	0.1904	6	0.210	0.210	0.210
Ca^2	2	0.2422	0.2422	0.2422				
Ba					2	0.210	0.210	0.210
S	2	0.000	0.000	0.000	2	0.000	0.000	0.000
Al	12	0.250	0.500	0.000	12	0.250	0.500	0.000
O^1	84	0.404	0.404	0.404	84	0.404	0.404	0.404
O^2	24	0.152	0.152	0.455	24	0.152	0.152	0.455

[a] The superscripts indicate the different positions of the Ca and O ions in the same unit cell.

TABLE 4

Lattice constants (Å) of the BF system

Sample	d	a	Sample	d	a
BF00	1.2645	9.290	BF06	1.2674	9.314
BF02	1.2654	9.299	BF08	1.2673	9.313
BF04	1.2666	9.307	BF10	1.2675	9.314

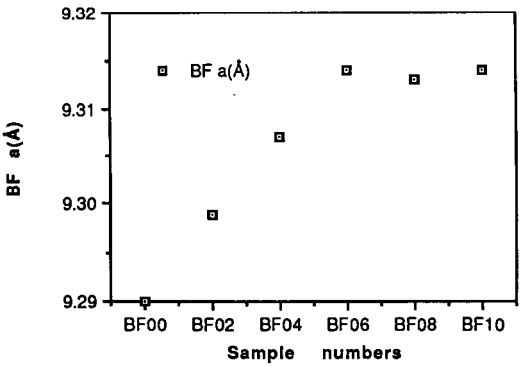

Fig. 1. The lattice constants of BF system compounds.

TABLE 5

XRD results of the BF system compounds [a]

	$3CaO \cdot 3Al_2O_3 \cdot BaSO_4$	C_xAF_{1-x} [b]	CA	$BaSO_4$
BF00	+ + + + +	n	T	T
BF02	+ + + + +	T	n	T
BF04	+ + + + +	+	n	T
BF06	+ + + +	+	n	T
BF08	+ + + +	+ +	n	T
BF10	+ + + +	+ +	n	T

[a] The more +, the larger the relative amount of that component; T, trace amount; n, not present.

[b] Mainly in the form of C_2F.

TABLE 6

Ferric oxide content in BF06 and BF08

Sample	Fe (wt.%)	Fe_2O_3 (wt.%)	Mol.% in the compound
BF06	3.73	5.32	0.285
BF08	3.78	5.39	0.289

TABLE 7

The compressive strengths of BF system compounds

Sample	SA ($cm^2\ g^{-1}$)	Comp. strength ($kg\ cm^{-2}$)		
		3 days	7 days	28 days
BF00	2391	644	714	919
BF04	2605	605	716	900
BF08	2540	596	707	916
BA	2400	825	940	1120
BA2	2760	767	920	1230

Although we know the maximum solid solution amount of ferric oxide in the compound, the exact situation of the iron atoms in the compound is still a problem. There are two types of replacements in the crystal lattice. In the first type, the atoms of the lattice are replaced directly; these are called Schottky defects. This kind of replacement makes the foreign atoms take part in the formation of the lattice. In the other type of defects, the minor atoms stay between the atoms of the lattice so that the foreign atoms do not take part in the formation of the lattice; these are called Frenkel defects. This is also a kind of bulk effect. The XRD results show that C_xAF_{1-x} (mainly in the C_2F form) is always formed in the mixture; therefore, there is always some ferric oxide left behind while some has reacted with the compound to form the first type of replacement, owing to the small difference between the radius of the Fe^{3+} ion (0.57 Å) and the Al^{3+} ion (0.47 Å). Therefore the second type of replacement dominates.

Strength and the process of hydration

The strengths of the compacts

Table 7 gives the compressive strengths of the BF system compounds while Figs. 2 and 3 show the plots of strength against time of aging. From

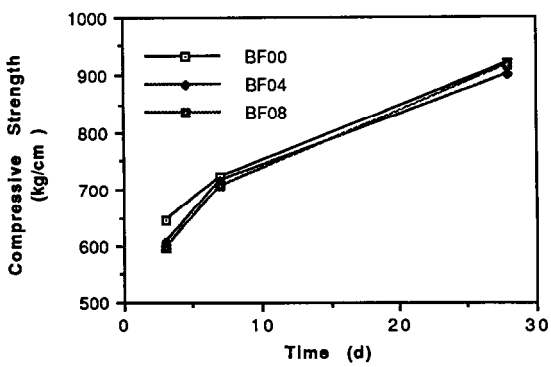

Fig. 2. Compressive strengths of BF00, BF04 and BF08.

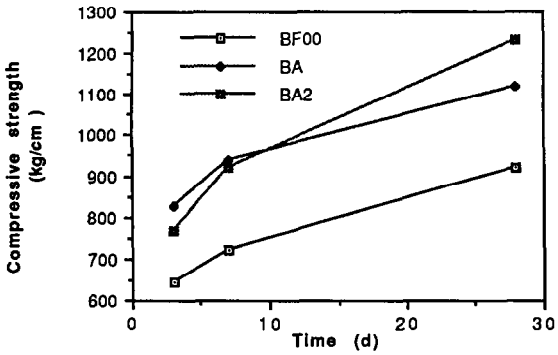

Fig. 3. Compressive strengths of BF00, BA and BA2.

the data, the early strengths of the compounds with ferric oxide are lower than that of the pure compound, BF00. But the later strengths can catch up with that of the pure compound. Also, when CA and CA_2 are added to the pure compounds corresponding to BA and BA2 samples, respectively, the early and later strengths are much larger than that of the pure compound. The reason for this is that the components CA and CA_2 in the BA and BA2 samples make the main contribution to the strength. In order to explain the growth of sample strengths, a study on the hydration is necessary.

The hydration process

Figures 4 and 5 show the hydration heat curves of the BF00 and BF06 samples, and the trends for the integration of hydration heat, respectively.

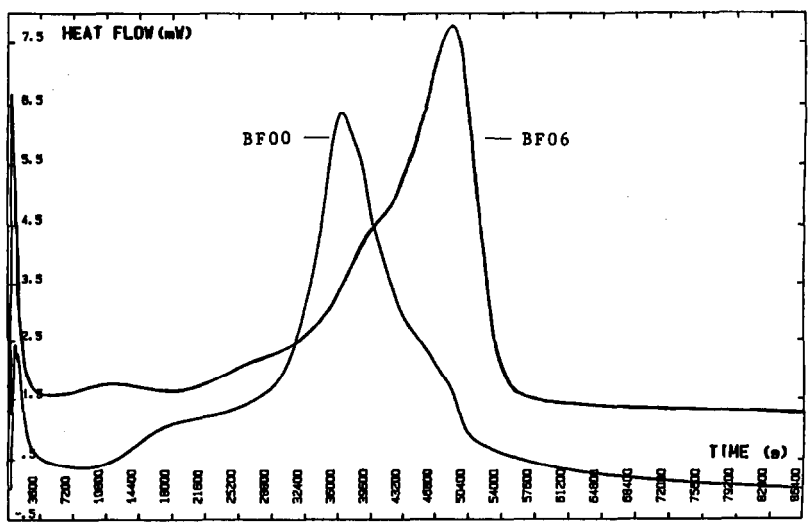

Fig. 4. The hydration curves of BF00 and BF06 samples.

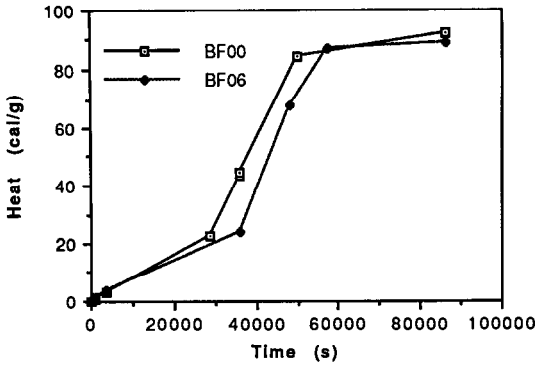

Fig. 5. The integrated hydration heats from the hydration heat curves.

By integration, the hydration heats before 1 h are 3.47 cal g^{-1} for BF00 and 3.96 cal g^{-1} for BF06, which means that the initial hydration rate of BF06 is faster than that of BF00. This phenomenon is due to the addition of ferric oxide into the compound $3CaO \cdot 3Al_2O_3 \cdot BaSO_4$, which makes it much more disordered (as mentioned above) and thus increases the reactivity. The C_xAF_{1-x} (mainly in C_2F form) which is present with the compounds but is relatively unreactive with water, makes the induction period of BF06 much longer than that of BF00. This is also due to the higher initial hydration rate and the fact that the hydration products appear

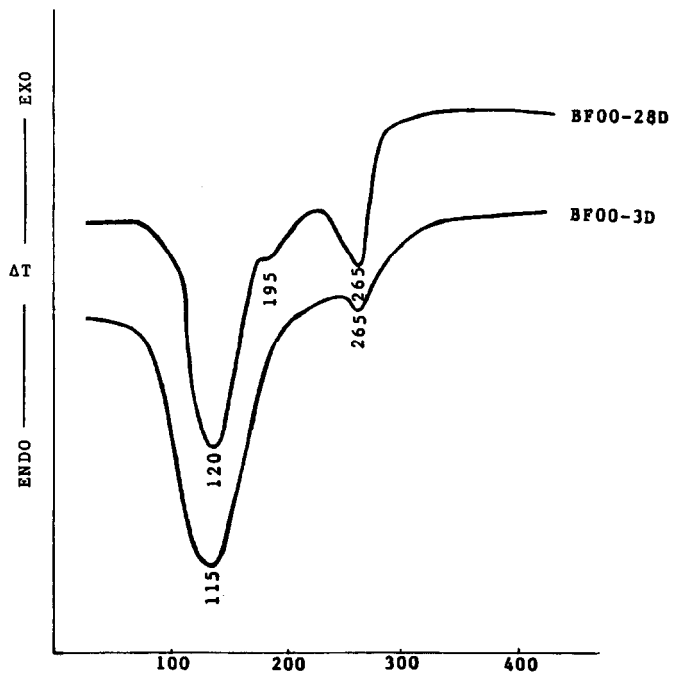

Fig. 6. The DTA curves of hydrated BF00 samples at 3 days and 28 days.

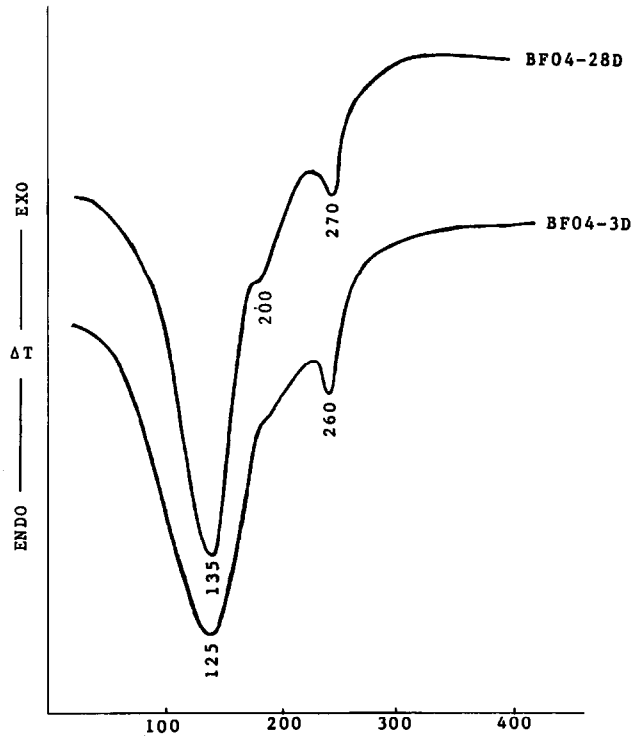

Fig. 7. The DTA curves of hydrated BF04 samples at 3 days and 28 days.

initially on the surface of the unreacted particles. The hydration process slowly progresses into the interior of the particles by diffusion as more water comes into contact with the unreacted particles. The total hydration heat of BF00, 92.08 cal g^{-1}, is higher than that of BF06, 89.03 cal g^{-1}. This is because C_xAF_{1-x} (mainly in C_2F form) is present in BF06.

The hydration products of various samples at different curing times, as determined by XRD, are shown in Table 8. Also Figs. 6–8 show the DTA patterns of selected samples. From these results and the previous research [3], the hydration can be seen to proceed as follows. When water is added to the sample, the main component ($3CaO \cdot 3Al_2O_3 \cdot BaSO_4$) quickly hydrates and releases Ca^{2+}, Al^{3+}, Ba^{2+} and SO_4^{2-} ions. The $BaSO_4$ crystallizes immediately and forms fine particles on the surface of the samples, owing to the very low dissociation constant ($K_{sp} = 1.1 \times 10^{-10}$) of $BaSO_4$. The diffusion rates of the Ba^{2+} and SO_4^{2-} ions are lower than those of the Ca^{2+} and Al^{3-} ions because of their larger sizes; therefore, this leads to the formation of $BaSO_4$ particles on the surface of samples. The small $BaSO_4$ particles settled on the surface of the unhydrated particles are shown in the SEM pictures, Figs. 9 and 10. Also the remaining CA component reacts rapidly with water to form calcium aluminate hydrates

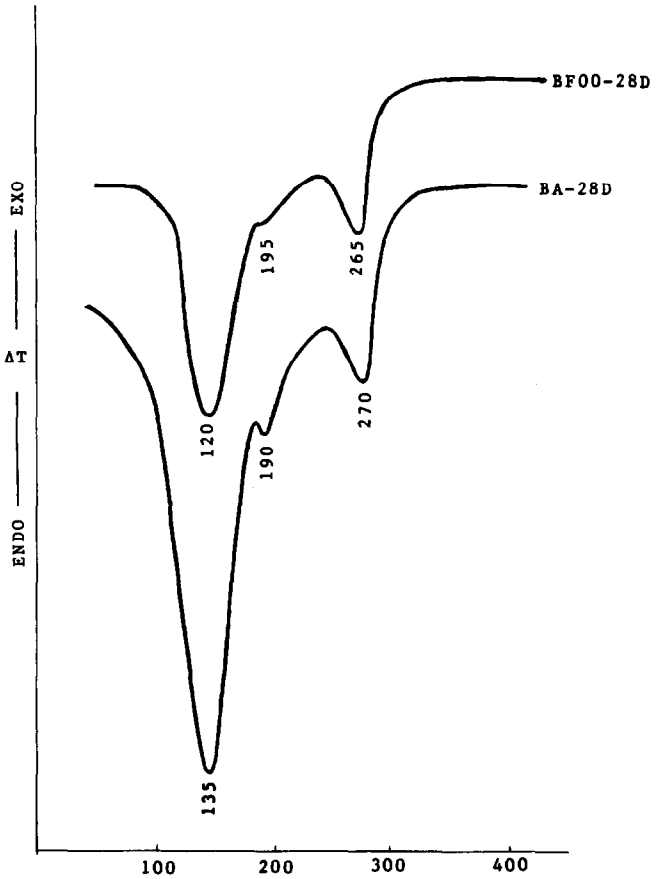

Fig. 8. The data curves of hydrated BF00 and BA samples at 28 days.

and aluminum gel. This is the initial stage of hydration and causes the first sharp peaks in the hydration heat curves, Fig. 4.

After the concentrations of ions in the liquid reach a certain level and sufficient hydration products cover the surface of the sample, the hydration process arrives at an induction or dormant period. In this dormant stage the diffusion process is very slow because of the covering of the sample surface by the hydration products and the common ion effect while the concentrations of ions are increasing. This is shown as the flat period in the hydration heat curves. The difference between the compounds with and without ferric oxide is similar to that of BF00 and BF06 (mentioned above).

When the concentrations of ions in the liquid reach another level, $BaSO_4$ and calcium aluminate hydrate crystallize again. The sudden drop in the concentrations of ions in the liquid phase and the contracting size of the unreacted particles are a result of the hydration accelerating the diffusion process. The hydration process then proceeds to an accelerating period. As the hydration progresses, the rate of the hydrolysis becomes faster than

TABLE 8

XRD results for the hydration products [a]

Sample	days	Unreacted	$BaSO_4$	CA	CA_2	CAH_{10}	AH_3	C_xAF_{1-x} [b]
BF00	3	+++++	++	–	–	T	+	–
	7	+++++	++	–	–	+	+	–
	28	++++	+++	–	–	++	++	–
BF04	3	+++++	++	–	–	T	+	T
	7	+++++	++	–	–	+	+	T
	28	++++	+++	–	–	++	++	T
BF08	3	+++++	++	–	–	T	+	+
	7	+++++	++	–	–	+	+	+
	28	++++	+++	–	–	++	++	+
BA	3	+++++	++	+++	–	+	+	–
	7	+++++	++	+++	–	+	+	–
	28	++++	++	++	–	++	++	–
BA2	3	+++++	++	–	+++	+	+	–
	7	+++++	++	–	+++	++	+	–
	28	++++	++	–	++	++	++	–

[a] The more +, the larger the relative amount of that component; T, trace amount.
[b] Mainly in the form of C_2F.

that of crystal growth which makes the concentrations of ions in the liquid phase reach another saturated level and causes the hydration process to slow down. This explanation indicates the reason for the appearance of the second flat period in the accelerating part of the hydration heat curves. At this time the unreacted samples become very small fragments and can react with water very easily. The hydration of these fragments is the final stage in the hydration process. This causes the final peaks in the hydration heat curves.

For the samples with and without ferric oxide, because C_xAF_{1-x} (mainly in C_2F form) is relatively unreactive, there is no great difference between the hydration processes. But when ferric oxide is present in the sample, the initial hydrated products have a larger porosity and thus cause the lower initial strengths. However, the process of hydration causes the pores to be filled which has little effect on their final strengths. The SEM figures show the difference in the porosity and interaction among the particles.

The DTA data analysis

In the DTA patterns, the peaks at around 120°C correspond to the dehydration of CAH_{10}, the peaks around 265°C correspond to the dehydration of AH_3, while the peaks around 195°C correspond to the dehydration of the compound which will be discussed in the following section.

In all the hydration products of the samples, no C_3AH_6 is present. From previous research [4], because the fine $BaSO_4$ particles have a strong ability to adsorb the calcium cations in the liquid it was shown that this prevents

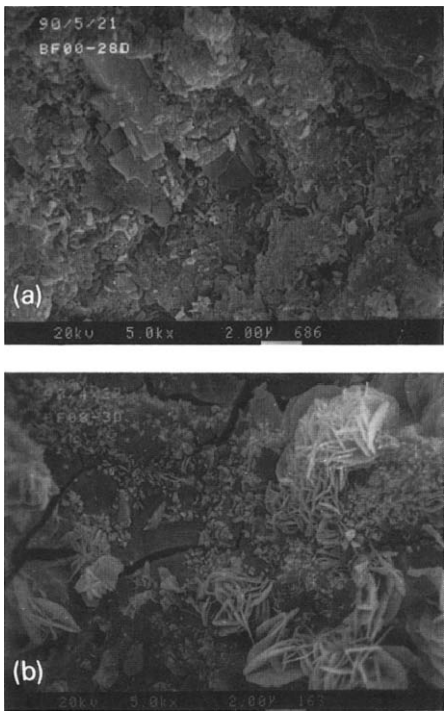

Fig. 9. Scanning electron micrographs at 5000×(original magnification): (a) hydrated BF00 sample at 28 days; (b) hydrated BF08 sample at 28 days. Note: small $BaSO_4$ particles are seen in both samples and hexagonal CAH_{10} can be seen in (b). A stronger interaction among the hydration products in (a) can be seen, in addition to the more porous hydration products in (b).

the transformation of CAH_{10} to C_3AH_6. This can prevent the decrease in the final strengths after hardening due to the formation of C_3AH_6, which would have caused a volume change. Thus a very encouraging prospect is presented here: high early and late strengths are produced in these cements with high barium and aluminum contents.

As mentioned in the previous research [4], there should be DTA peaks for C_2AH_8 (142°C) instead of the small peaks around 190°C which are shown in Figs. 6–8. This is very obvious with the BA-28D sample and it appears as small shoulders in BF00-28D, BF04-3D and BF04-28D. From other references [5,6], the peaks around this temperature in the hydrates of calcium aluminosulfate, $3CaO \cdot 3Al_2O_3 \cdot CaSO_4$, correspond to the calcium monosulfoaluminate hydrate, $3CaO \cdot Al_2O_3 \cdot CaSO_4 \cdot 12H_2O$. In the BF system these peaks may correspond to similar hydrates which are composed of CaO, Al_2O_3, H_2O and $BaSO_4$ instead of $CaSO_4$. The reason for this phenomenon is that the hydration conditions of the previous research [4] were $w/c = 0.40$, which is higher than that in this paper, $w/c = 0.29$. Due to the lower w/c ratio used in the present research, the concentrations of ions in the liquid phase are somewhat higher and this will make the particle

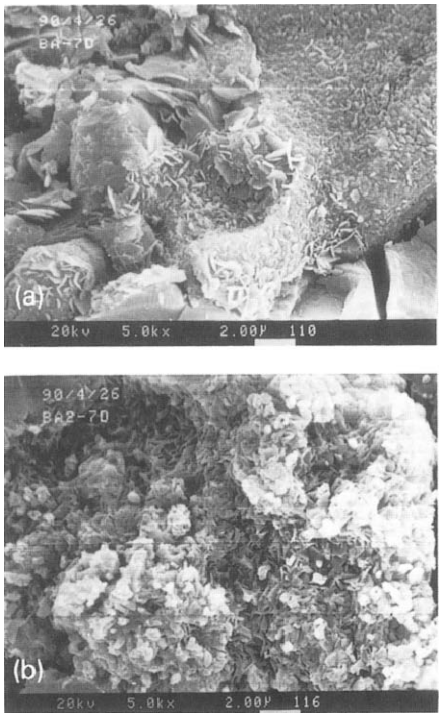

Fig. 10. Scanning electron micrographs at 5000×(original magnification): (a) hydrated BA sample at 7 days; (b) hydrated BA2 sample at 7 days. Note: small $BaSO_4$ particles and hexagonal CAH_{10} can be seen in both samples. They show a very strong interaction among the hydration products.

size much smaller and give a higher surface area as well as reactivity. When there are some calcium cations and aluminum cations present in the liquid while $BaSO_4$ is forming, they can form a compound which is similar to the calcium monosulfoaluminate hydrate. Also because of the difference in the w/c ratio, the peaks presented in this paper have higher temperatures than those in previous research.

There are position changes in the peaks at around 120°C, 265°C and 190°C for different samples at different curing periods. For BF00, for example, the peak at around 120°C which corresponds to CAH_{10} is at 120°C after 28 days, which is higher than that of samples aged for 3 days which is at 115°C. This is due to the better crystal form of CAH_{10} which is caused by the further growth of the crystal with aging. For the same reason, the shape of the peaks at 28 days is sharper than those at 3 days. For samples of the same curing age, the temperature order of the peak at round 120°C is BA = BF04 > BF00; at around 265°C, BA > BF04 = BF00. The reason for these orders is also due to the difference in the hydration and crystal forms among these samples. The peak at around 190°C is not shown by sample BF00-3D but is present for sample BF04-3D. This

indicates that the initial hydration process of BF04 (with ferric oxide) is faster than that of BF00 (without ferric oxide), as mentioned above when discussing the hydration process.

CONCLUSIONS

The structure of $3CaO \cdot 3Al_2O_3 \cdot BaSO_4$ was determined from its powder X-ray diffraction pattern using computer programs, based on the structure of $3CaO \cdot 3Al_2O_3 \cdot CaSO_4$ as determined using a single crystal. The structure is T^5-I23; $a = b = c = 9.303 \pm 0.002$ Å and $\alpha = \beta = \gamma = 90°$.

The maximum amount of solid solution of ferric oxide in $3CaO \cdot 3Al_2O_3 \cdot BaSO_4$ is about 5.36 wt.% and the proposed formula of the maximum solid solution of ferric oxide is $3CaO \cdot 2.71Al_2O_3 \cdot 0.29Fe_2O_3 \cdot BaSO_4$.

The addition of ferric oxide causes a slight decrease in the compressive strength which is due to the formation of C_xAF_{1-x} (mainly in the C_2F form).

The hydration processes of $3CaO \cdot 3Al_2O_3 \cdot BaSO_4$ are:

$$3CaO \cdot 3Al_2O_3 \cdot BaSO_4 + H_2O \rightarrow 3(CaO \cdot Al_2O_3) + BaSO_4 + H_2O$$

$$CaO \cdot Al_2O_3 + 10H_2O \rightarrow CaO \cdot Al_2O_3 \cdot 10H_2O$$

$$CaO \cdot Al_2O_3 + BaSO_4 + nH_2O \rightarrow \text{compound similar to}$$

$$\text{calcium monosulfoaluminate hydrate} + Al_2O_3 \cdot 3H_2O$$

Under the hydration conditions of this paper, this is the first time that there has been shown to be a compound present with a DTA peak at 190–200°C which is very similar to that of calcium monosulfoaluminate hydrate. As mentioned, these two compounds may have similar formulae.

The presence of $BaSO_4$ prevents the transformation of CAH_{10} to C_3AH_6 (which would have caused a reduction in strength). This property makes possible the manufacture of high early- and final-strength aluminum–barium cements.

The initial hydration processes of compounds with ferric oxide are faster than that of the compound without ferric oxide, while the total hydration heat of the compound without ferric oxide is higher.

ACKNOWLEDGMENTS

All the work was performed under the guidance of Prof. Dr. X.J. Feng who taught D.C. not only how to do research but also how to be a man and to pursue a career in life. He was much more to D.C. than an advisor. We are also very appreciative of our colleagues, Dr. Hu Shuguang, Mr. Liao, etc., who helped with the difficult experiments. Thanks are also due to Prof. Shun and Ms. Zhang of the Testing Center in the Wuhan University

of Technology who did the hard work of analyzing the structure of $3CaO \cdot 3Al_2O_3 \cdot BaSO_4$.

REFERENCES

1 I. Teoreanu, M. Muntean and I. Dragnea, Cemento, 83(1) (1986) 39–46.
2 X.J. Feng, G.L. Liao and S.Z. Long, 4th Academic meeting on cement, Vol. 4, Chinese Silicate Society, Beijing, 1987.
3 G.L. Liao, M. Sc. Thesis, Wuhan University of Technology, 1986.
4 X.J. Feng and S.Z. Long, Report of the Chinese Silicate Society, Hubei, People's Republic of China, 1989.
5 V.S. Ramachandran, Application of DTA in Cement Chemistry, Chemical Publish. Co. Inc., New York, 1969.
6 M. Murat, Proc. Int. Seminar on Calcium Aluminates, Turin, 1982, Politechnico di Torino, Turin, Italy, 1982, pp. 59–84.